Gemmological and Spectroscopic Characteristics of Different Varieties of Amber from the Hukawng Valley, Myanmar

Xinran Jiang, Zhiqing Zhang, Yamei Wang and Fanli Kong

ABSTRACT: With its broad range of varieties, Burmese amber may show various optical effects, including 'oil gloss' (a red or green surface fluorescence effect) and phosphorescence phenomena. Samples representing golden, brown, red ('blood'), 'beeswax' and 'root' ambers were characterised, as well as those showing red or green 'oil gloss'; many of these also displayed phosphorescence. Common internal features seen with optical microscopy include reddish brown dot-like inclusions in brown amber and flow-banded concentrations of bubbles in 'beeswax' and 'root' ambers (the latter displaying patterns comprised of opaque light- and dark-coloured layers). SEM imagery revealed various scaly or layered structures on freshly broken surfaces, micro-bubbles in some samples and distinctive hollow micro-channels in 'root' amber. Fluorescence spectra recorded luminescence centres at 432 and 470 nm in all samples, and additionally at 650 nm (± 625 nm) in red 'oil gloss' amber. The 'oil gloss' appearance is caused by a mixture of surface fluorescence and the amber's body colour. Phosphorescence spectroscopy showed that the effect was strongest at 525 nm, and the phosphorescence lifetime measured at this emission wavelength ranged from 0.134 to 1.396 seconds.

Myanmar is a major source of Asian amber (e.g. Figure 1), and Burmese amber (or Burmite) has the longest geological history (about 98 million years old: Shi *et al.* 2012) and most complicated formational patterns compared to material from other localities around the world (Edwards *et al.* 2007; Dutta *et al.* 2011; Zong *et al.* 2014). For millennia, Burmese amber has been highly valued for producing art objects and jewellery (Zherikhin & Ross 2000), and according to the authors' research it currently represents 10%–20% of China's amber market. Burmese amber is also well known for its diversity of inclusions, including invertebrates and plant materials (Laurs 2012; Lu *et al.* 2014), which have multidisciplinary importance to fields such as geology, biology and palaeontology (e.g. Xing *et al.*

2016). Most Burmese amber comes from the Hukawng Valley in northern Myanmar (e.g. Cruickshank & Ko 2003), although other deposits are known near Khamti in the Sagaing Region of northern Myanmar (Liu 2018) and near Hti Lin in the central part of the country (Tay *et al.* 2015).

Several distinctive types of amber are recognised from Myanmar, and some of them have not been found elsewhere. However, their gemmological properties and fluorescence characteristics have not been studied systematically until fairly recently (see Jiang *et al.* 2017, 2018, 2019; Xie *et al.* 2017; Xiao & Kang 2018—all in Chinese). In this study, we characterise different types of Burmese amber by observing their micro-structures as well as fluorescence and phosphorescence spectra to explain their appearance and optical effects.

Figure 1: This large faceted Burmese amber weighs 42.33 ct and shows the attractive appearance of golden amber from Myanmar. Photo by Mark Smith, Thai Lanka Trading Ltd. Part., Bangkok, Thailand.
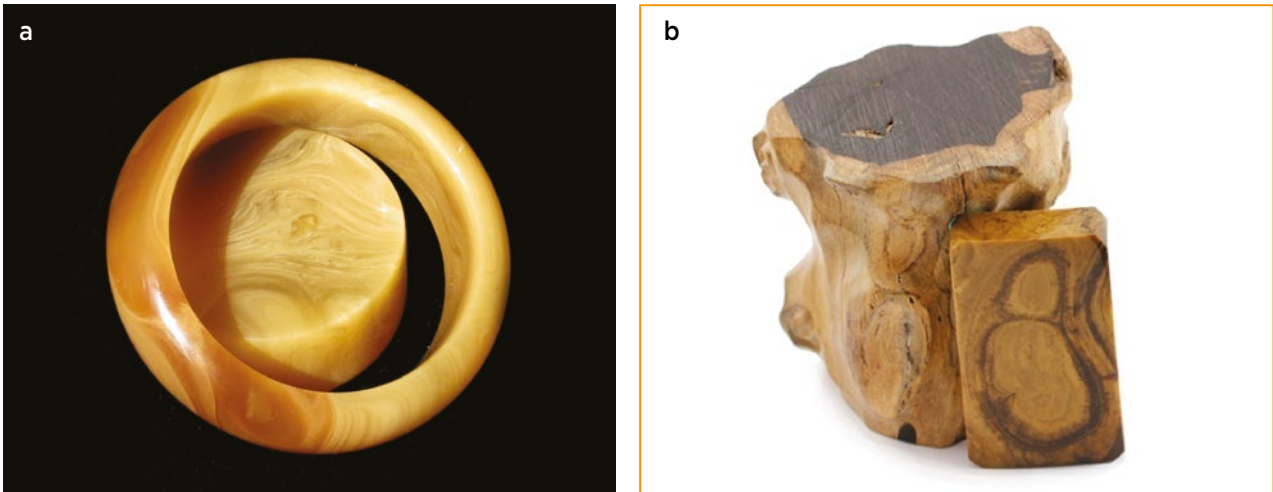
Types of Burmese Amber

Burmese amber can be broadly divided into two main groups, according to whether it is mostly transparent or opaque. The mostly transparent ambers are classified according to their colour into golden, brown and red (or 'blood') varieties (Figures 2a–c), with brown being the most common. The red colour of 'blood' amber is caused by oxidation and is concentrated near the surface; when such material is sliced, the golden colour of the interior becomes visible (Figure 2d). If the coloured layer is particularly dark, it is called 'black' amber (Xiao *et al.* 2014; Zhang *et al.* 2017).

There are two main opaque types of amber found in Myanmar: 'beeswax' amber, which is a mixture of opaque and transparent ambers displaying flow patterns (Figure 3a); and 'root' amber, which shows a mixture of colours (e.g. white, yellow, brownish yellow, orange and/or brown) in patterns that resemble wood or tree roots (Figure 3b).

Some transparent ambers display an 'oil gloss' surface fluorescence effect when observed in sunlight and under some artificial light sources. These samples may show various body colours when viewed over a white background (yellow, greenish yellow, brown and brownish
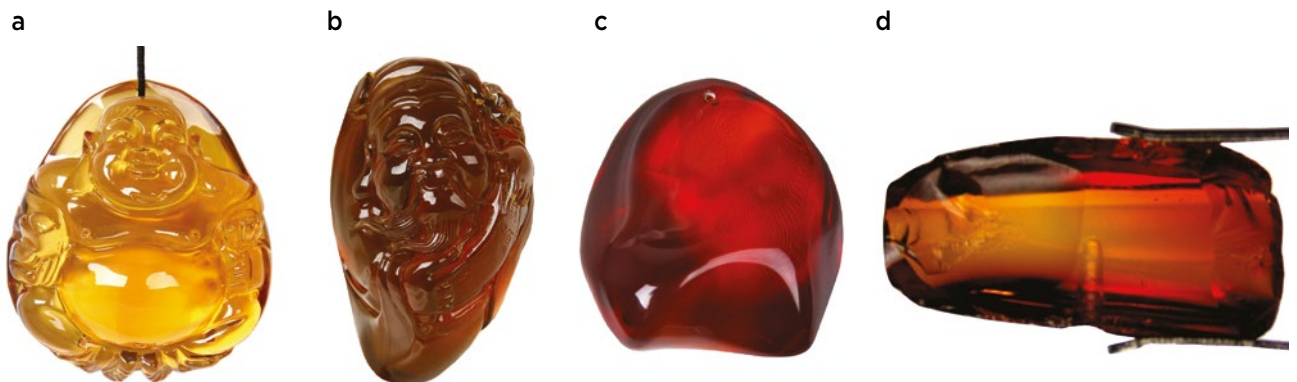
Figure 2: Transparent Burmese amber may be divided into various colour categories, such as (**a**) golden, (**b**) brown, which is the most common colour variety, and (**c**) 'blood' or red amber. (**d**) When 'blood' amber is sliced, the golden colour of the interior becomes visible, since the red colouration is only present near the surface. The samples weigh (a) 156.15 ct, (b) 146.60 ct, (c) 105.60 ct and (d) 2.83 ct. Photos a–c reprinted with permission from Wang (2018); image d by X. Jiang.

Figure 3: The two types of opaque Burmese amber consist of (**a**) 'beeswax' and (**b**) 'root' varieties. The total weight of the samples is (a) 78.77 g and (b) 25.20 g. Photos reprinted with permission from Wang (2018).

red), but appear to exhibit different surface hues over a black background. For example, amber with a greenish yellow body colour may show a reddish surface appearance when viewed against a black background (Figure 4a, b). Also, reddish brown amber can show a greenish surface appearance against a black background (Figure 4c), and is therefore sometimes known colloquially as 'chameleon' amber. Such amber is often referred to in

China as having 'machine-oil gloss' because its appearance may resemble that of machine oil.

Burmese amber may also show phosphorescence. After being illuminated by bright light for a certain time period (typically at least several seconds), the exposed area will display greenish yellow phosphorescence for a short time (typically 0.5–1 s; see Figure 4d). This phenomenon may occur in various types of transparent
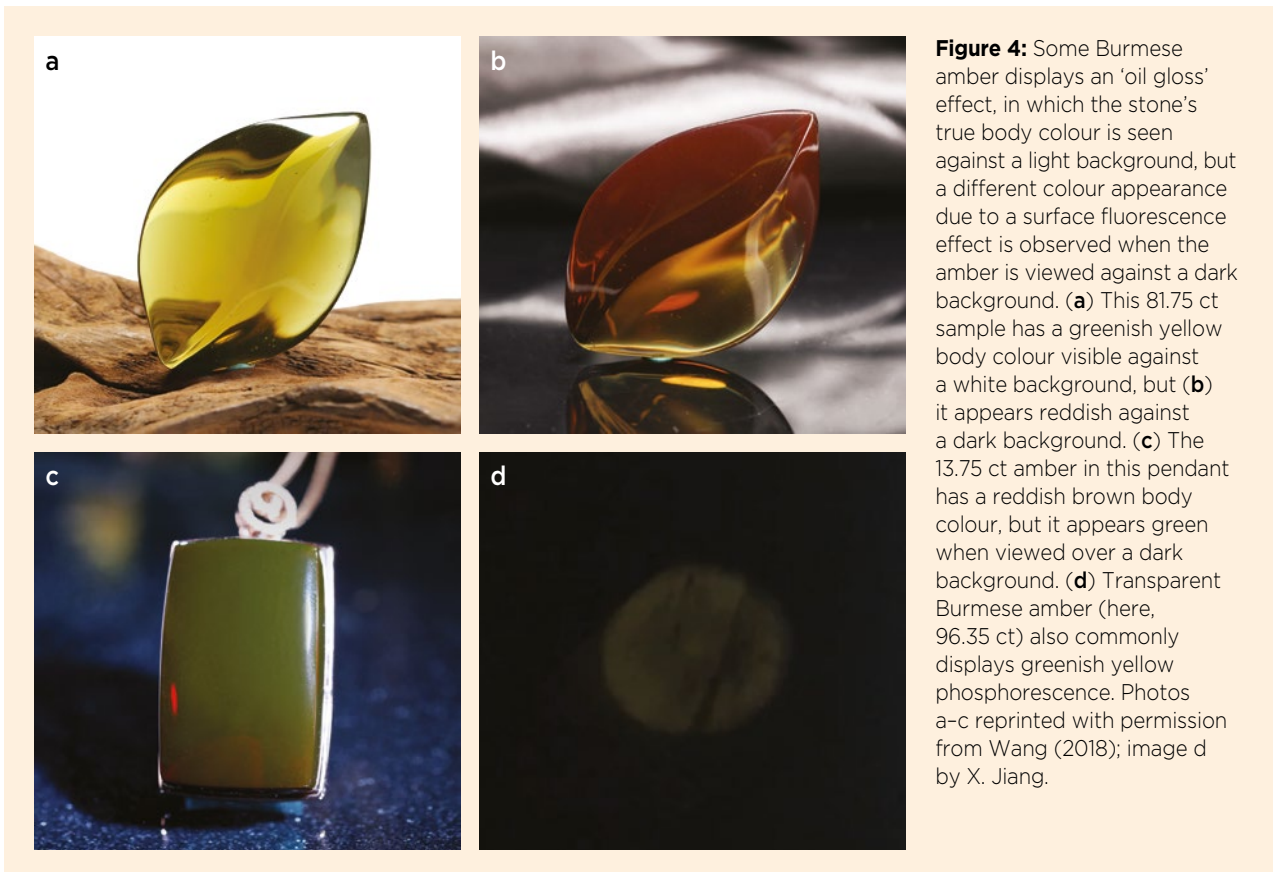
Figure 4: Some Burmese amber displays an 'oil gloss' effect, in which the stone's true body colour is seen against a light background, but a different colour appearance due to a surface fluorescence effect is observed when the amber is viewed against a dark background. (**a**) This 81.75 ct sample has a greenish yellow body colour visible against a white background, but (**b**) it appears reddish against a dark background. (**c**) The 13.75 ct amber in this pendant has a reddish brown body colour, but it appears green when viewed over a dark background. (**d**) Transparent Burmese amber (here, 96.35 ct) also commonly displays greenish yellow phosphorescence. Photos a–c reprinted with permission from Wang (2018); image d by X. Jiang.

Figure 5: This light yellow Burmese amber (**a**) appears greenish in daylight-equivalent lighting (**b**) due to its blue long-wave UV fluorescence (**c**). The sample weighs 20.21 ct; photos by X. Jiang.

Burmese amber and is commonly known as a 'glow-in-the-dark' effect.

Pale-coloured Burmese amber with blue fluorescence may appear green (from the combination of blue luminescence and yellow body colour; see Figure 5) or even blue when viewed in daylight, and is therefore sometimes called 'blue' amber; such material is known from various world localities and has been well documented (e.g. Chekryzhov *et al.* 2014; Jiang *et al.* 2017), so it is not included in the present article.

MATERIALS AND METHODS

Samples

Nine representative amber samples from the Hukawng Valley in Myanmar were studied for this report (see Table I and Figure 6). These included three pieces of transparent amber (golden, brown and 'blood'), both types of opaque amber (one 'beeswax' piece and two 'root' samples) and three 'oil gloss' ambers (two showing red 'oil gloss' and one with green 'oil gloss'). Phosphorescence was exhibited by most samples, but not by the three opaque pieces or the 'blood' amber.

Table I: General gemmological characteristics of the nine Burmese amber samples.

Type	Sample ID	Body colour	Optical effects	Transparency	SG	Internal features
Golden amber	JP	Golden	Phosphorescence	Transparent	1.04	Reddish brown impurities and calcite-filled fissures
Brown amber	ZP	Reddish brown	Phosphorescence	Mostly transparent	1.04	Reddish brown dot-like inclusions directionally arranged along flow patterns
'Blood' amber	XP	Red (surface)	—	Transparent	1.05	No features seen
'Beeswax' amber	ML	Yellowish white	—	Opaque	1.04	Yellowish white flow patterns, black inclusions
'Root' amber	GP-1	Yellowish white and yellowish brown	—	Mostly opaque	1.02	Conspicuous yellowish white flow patterns with opaque and transparent zones
	GP-2	Yellowish white	—	Opaque	1.04	Mottled structure
'Oil gloss' amber	GX-1	Reddish brown	Red 'oil gloss', phosphorescence	Transparent	1.03	Fissures resembling a bird feather or displaying iridescence
	GX-2	Greenish yellow	Red 'oil gloss', phosphorescence	Transparent	1.03	Nearly free of inclusions
	GX-3	Reddish brown	Green 'oil gloss' (or 'chameleon'), phosphorescence	Transparent with opaque impurities	1.05	Dark opaque impurities (foreign objects)

Figure 6: Burmese amber samples studied for this report include (**a**) golden, (**b**) brown, (**c**) 'blood', (**d**) 'beeswax', (**e** and **f**) 'root', (**g** and **h**) red 'oil gloss' and (**i**) green 'oil gloss' varieties. The colour appearance of the 'oil gloss' varieties is shown against both white and black backgrounds. Photos by X. Jiang.

Experimental Methods and Test Conditions

Internal features in all samples were examined with a gemmological microscope. In addition, the structural characteristics in five of the samples—consisting of the golden, brown and 'beeswax', as well as the two 'root' ambers—were studied with scanning electron microscopy (SEM), which was performed at the State Key Laboratory of Geological Processes and Mineral Resources, China University of Geosciences, Wuhan. The samples were fractured and gold coated to provide surfaces suitable for SEM examination (cf. Zhang & Li 2010). We used an FEI Quanta 200 environmental SEM operating under low vacuum with the following conditions: 20 kV acceleration voltage, 3.5 nm electron beam spot diameter, 1024 × 884 pixels resolution and 12.5–18.3 mm working distance.

Infrared spectroscopy of all samples was performed at the Guangzhou laboratory of the Gemmological Institute, China University of Geosciences. The specular reflection method was used (Kramers-Kronig transformation) with a Bruker Tensor 27 Fourier-transform infrared (FTIR) spectrometer under the following conditions: 220 V scanning voltage, 6 mm raster, 10 kHz scanning rate, 32 scans, 4000–400 cm^{-1} range and 4 cm^{-1} resolution.

The fluorescence of all samples was checked with a standard 4 W long-wave UV lamp. Three-dimensional fluorescence spectroscopy was performed on the five samples showing fluorescence (JP, ZP, GX-1, GX-2 and GX-3) with a Jasco FP-8500 spectrofluorometer at the Gem Testing Center, China University of Geosciences, Wuhan. The parameters included a bandwidth excitation of 5 nm and emission of 5 nm, response time of 10 ms, excitation range of 220–500 nm (5 nm interval), emission range of 240–750 nm (1 nm interval) and scanning velocity of 2,000 nm/min. The data were plotted according to excitation wavelength, emission wavelength and fluorescence intensity, and in addition we generated two-dimensional fluorescence spectra (emission wavelength vs. intensity) for the optimum excitation wavelength of 365 nm and for other excitations (400 and 460 nm). For comparison, we also obtained two-dimensional fluorescence spectra for samples GX-1 and GX-2 with another instrument, a Qspec photoluminescence microspectrometer (405 nm excitation), at the Guangzhou laboratory of the Gemmological Institute, China University of Geosciences.

Transient phosphorescence time-resolved spectroscopy was performed on the same five samples at the Hubei Key Laboratory of Low Dimensional Optoelectronic Materials and Devices, Xiangyang, using an Edinburgh Instruments FLS980 steady-state and transient fluorescence spectrometer with a 60 W xenon lamp (365 nm) as the excitation source. We measured the time-resolved phosphorescence spectra and the phosphorescence lifetime of each sample. The parameters included an emission range of 420–650 nm, test frequency of 100 Hz, monochromatic bandwidth excitation of 20 nm, luminous flux of 1,000, test time-frame of 8 s, trigger delay time of 0.1 ms, step size of 5 nm and a test time at each fixed wavelength of 1 min. The optimum monitoring wavelength for each sample was determined from the results of the transient phosphorescence time-resolved spectra, and the phosphorescence lifetime was then measured at that wavelength (525 nm). Each phosphorescence lifetime test had a frequency of 100 Hz, monochromatic bandwidth excitation of 20 nm, luminous flux of 1,000, test time frame of 4 s and trigger delay time of 0.1 ms. Each test utilised a total of 5,000 photons.

RESULTS

Optical Microscopy: Internal Features

The golden amber showed reddish brown impurities (Figure 7a) and surface-reaching fissures that were filled with a white mineral showing good cleavage (probably calcite; Figure 7b). The brown amber contained concentrations of reddish brown dots that were directionally arranged, resulting in dark flow patterns (Figure 7c). The 'blood' amber sample did not contain any inclusions, and there was no evidence that its red colour was created artificially by heating in the laboratory.

The 'beeswax' amber showed obvious flow patterns, with lighter-coloured bands containing large amounts of bubbles (Figure 7d; cf. Wang *et al.* 2016), as well as black inclusions (Figure 7e). The 'root' amber showed two different types of features: (1) distinctive yellowish white flow patterns that were locally concentric, with well-defined borders between transparent and opaque zones (sample GP-1; see Figure 7f), and (2) a mottled structure (sample GP-2; see Figure 7g).

Of the three samples showing the 'oil gloss' effect, GX-1 contained fissures that in one case resembled a bird feather (Figure 7h) or locally displayed iridescence. Sample GX-2 was nearly free of inclusions, while GX-3 contained some dark impurities (Figure 7i) but lacked the reddish brown dot-like inclusions.
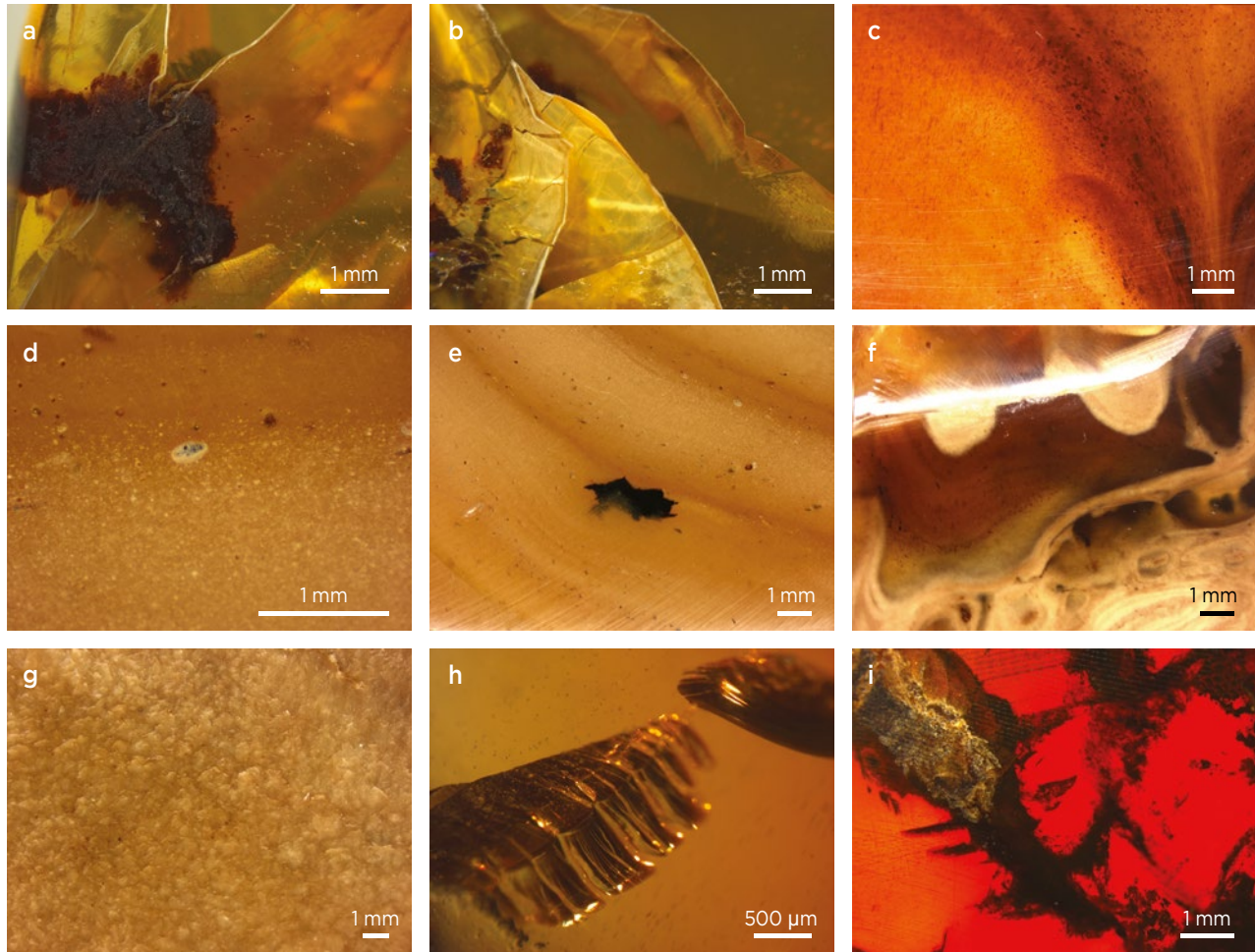
Figure 7: Various types of internal features are seen in the Burmese amber samples examined for this report. The golden amber contains (**a**) reddish brown impurities and (**b**) fractures that are probably filled with calcite. (**c**) The brown amber shows abundant reddish brown dot-like inclusions in a flow-banded arrangement. Internal features in 'beeswax' amber consist of (**d**) abundant bubbles or (**e**) flow patterns and dark inclusions. 'Root' amber may display (**f**) conspicuous flow patterns or (**g**) a mottled structure. (**h**) 'Oil gloss' sample GX-1 contains a fissure resembling a bird feather, while (**i**) GX-3 contains dark impurities. Photomicrographs by X. Jiang.

Electron Microscopy: Structural Characteristics

SEM examination of the golden amber showed a scaly, layered appearance with no bubbles (Figure 8). The surface of the brown amber was smoother, and the dot-like inclusions (which appeared reddish brown with optical microscopy; see Figure 7c) were directionally oriented along flow patterns. The individual dot-like inclusions had oval shapes (Figure 9a) and were of various sizes. Higher magnification of these inclusions revealed that they commonly contained an inhomogeneous texture (Figure 9b), consisting of smooth oval areas within a slightly more scaly-appearing matrix (Figure 9c, d).

The 'beeswax' amber contained locally abundant bubbles along flow layers that corresponded to the lighter-coloured, more opaque bands (Figure 10a, b). The flow layers were probably caused by external
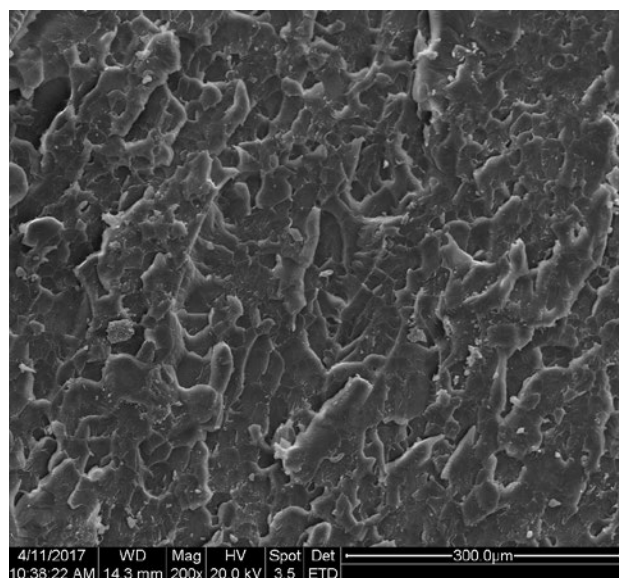
Figure 8: SEM imagery of the golden amber sample reveals a scaly, layered structure. Image by X. Jiang.
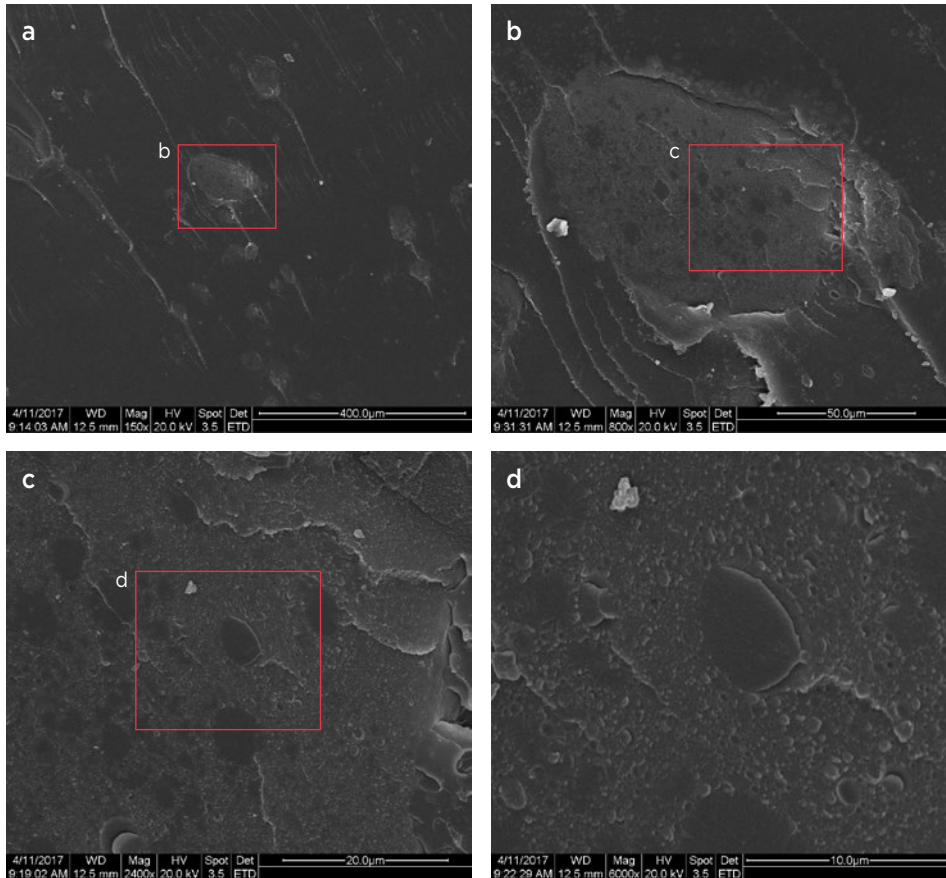
Figure 9: The structure of the reddish brown dot-like inclusions in the brown amber is shown in these successively higher-magnification SEM images, taken at (**a**) 150×, (**b**) 800×, (**c**) 2,400× and (**d**) 6,000×. Images by X. Jiang.

temperature and pressure during burial of the amber, which led to mutual extrusions between adjacent bubbles. The darker, more transparent layers in the 'beeswax' amber lacked bubbles but still showed some evidence of flow layering (Figure 10c).

The two samples of 'root' amber revealed different characteristics. A lighter-coloured, opaque area of sample GP-1 (Figure 11a) contained micro-bubbles showing various shapes and sizes, along with thin, curved, hollow micro-tubes (Figure 11b, right side of image). In some cases, the bubbles occurred alongside the tubes. A layered structure was also observed in the areas containing the bubbles and tubes. An adjacent, more transparent area of this sample appeared mostly featureless in the SEM (Figure 11b, left side). 'Root' amber sample GP-2 was examined in a mottled area that was free of consistent flow patterns (Figure 12). The SEM images showed a fine-grained scaly appearance along with elliptical bubbles of various size, although they were significantly less abundant than in GP-1.
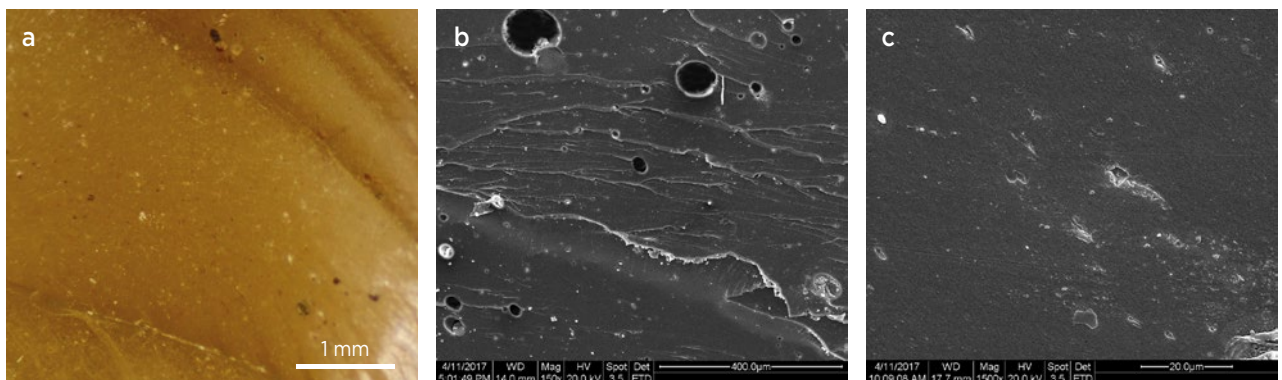
Figure 10: A closer look at the 'beeswax' amber (**a**) with the SEM reveals the microstructure of an opaque zone (**b**), which contains bubbles of various size, and a transparent zone (**c**), which has a more featureless structure. Both areas show flow patterns. Photomicrograph and SEM images by X. Jiang.
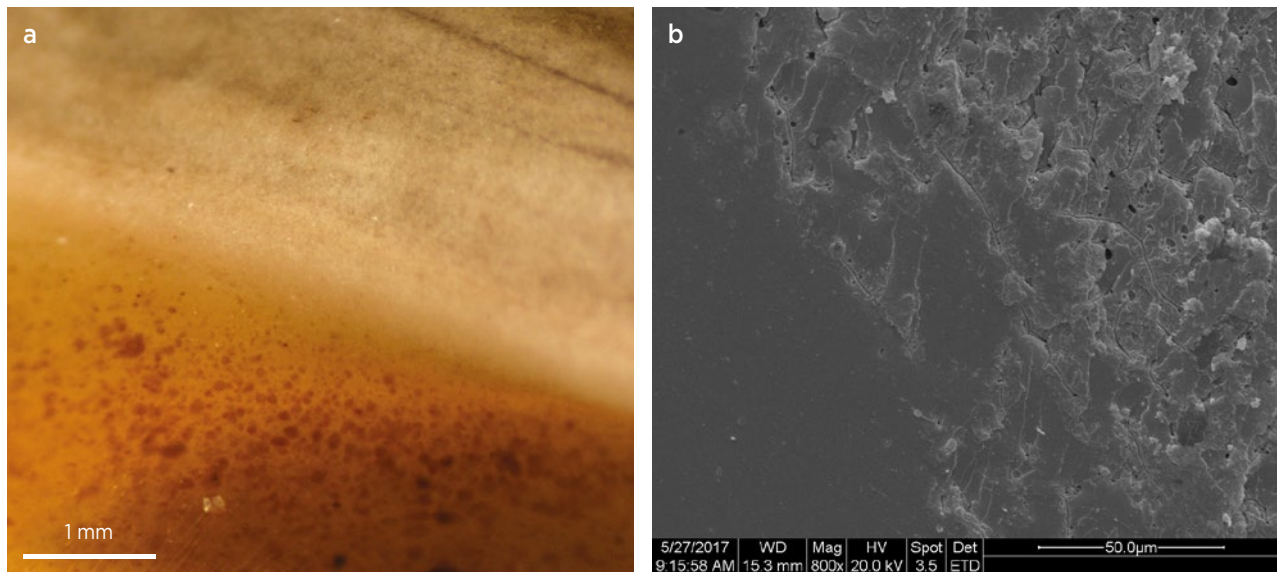
Figure 11: The transitional zone between transparent (lower left) and opaque (upper right) areas of 'root' amber sample GP-1 (**a**) is shown in this SEM image (**b**). The transparent portion appears smooth and featureless, while the opaque zone displays a layered structure with curved hollow micro-tubes between the layers that are locally associated with bubbles. Photomicrograph and SEM image by X. Jiang.
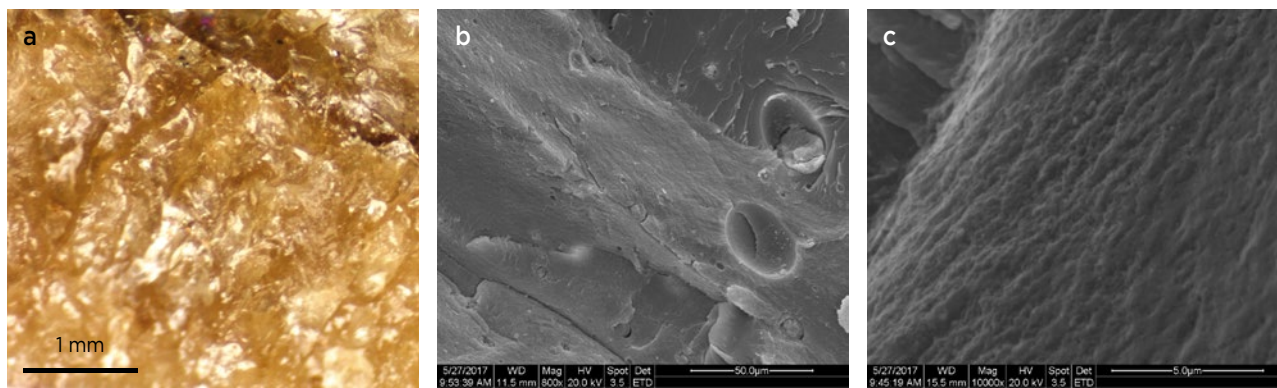
Figure 12: Examination of the mottled area of 'root' amber sample GP-2 (**a**) with the SEM reveals (**b**) heterogeneous surface features with elliptical bubbles of various size and (**c**) a fine-scaly microstructure. Photomicrograph and SEM images by X. Jiang.

Infrared Spectroscopy

The FTIR spectra were highly consistent among the different types of Burmese amber samples that were analysed (Figure 13). Strong bands at around 2928–2930 cm^{-1} and at 2862 cm^{-1} were caused by asymmetric C–H stretching vibrations. Stretching vibrations of the carbonyl (C=O) functional group caused a band at around 1719–1722 cm^{-1}. The bands at 1458 and 1375 cm^{-1} were caused by CH_2–CH_3 and symmetric deformation vibrations, respectively. Thus, the amber was confirmed to be an aliphatic compound, and the bands at 1027–1034 and 972 cm^{-1} were caused by lipid C–O–C and C–O stretching vibrations, respectively (Marrison 1951; Lambert & Frye 1982; Abduriyim *et al.* 2009; Wang *et al.* 2015, 2017; Lan *et al.* 2017).

Fluorescence and Phosphorescence

The golden and brown ambers displayed violetish blue long-wave UV fluorescence (Figure 14a, b), which is the most common luminescence colour in Burmese amber. The two samples displaying a red 'oil gloss' effect showed a peculiar magenta or violetish purple fluorescence (Figure 14c, d), while the amber displaying green 'oil gloss' showed whitish blue luminescence (Figure 14e).

The 'blood' amber and the opaque samples were inert to long-wave UV radiation, and they were also inert to the 220–500 nm excitation range utilised for fluorescence spectroscopy. Greenish yellow phosphorescence was noted in all of the transparent samples except for the 'blood' amber.
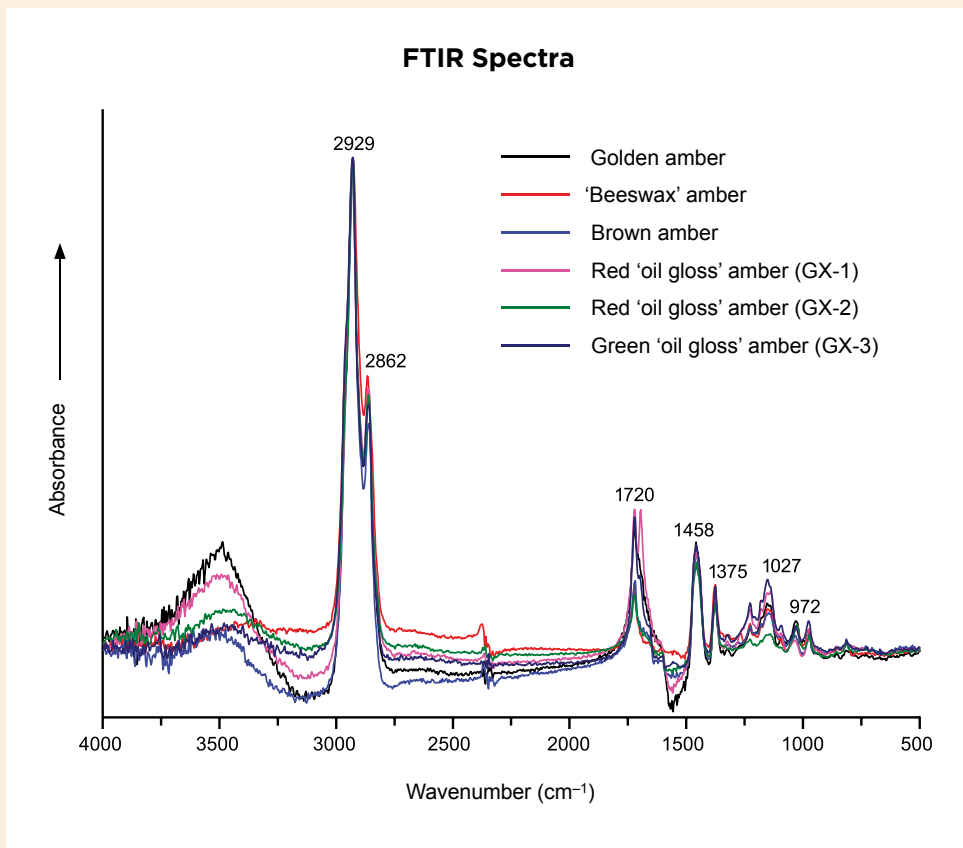
Figure 13: FTIR spectra of the six analysed specimens of Burmese amber show similar features.
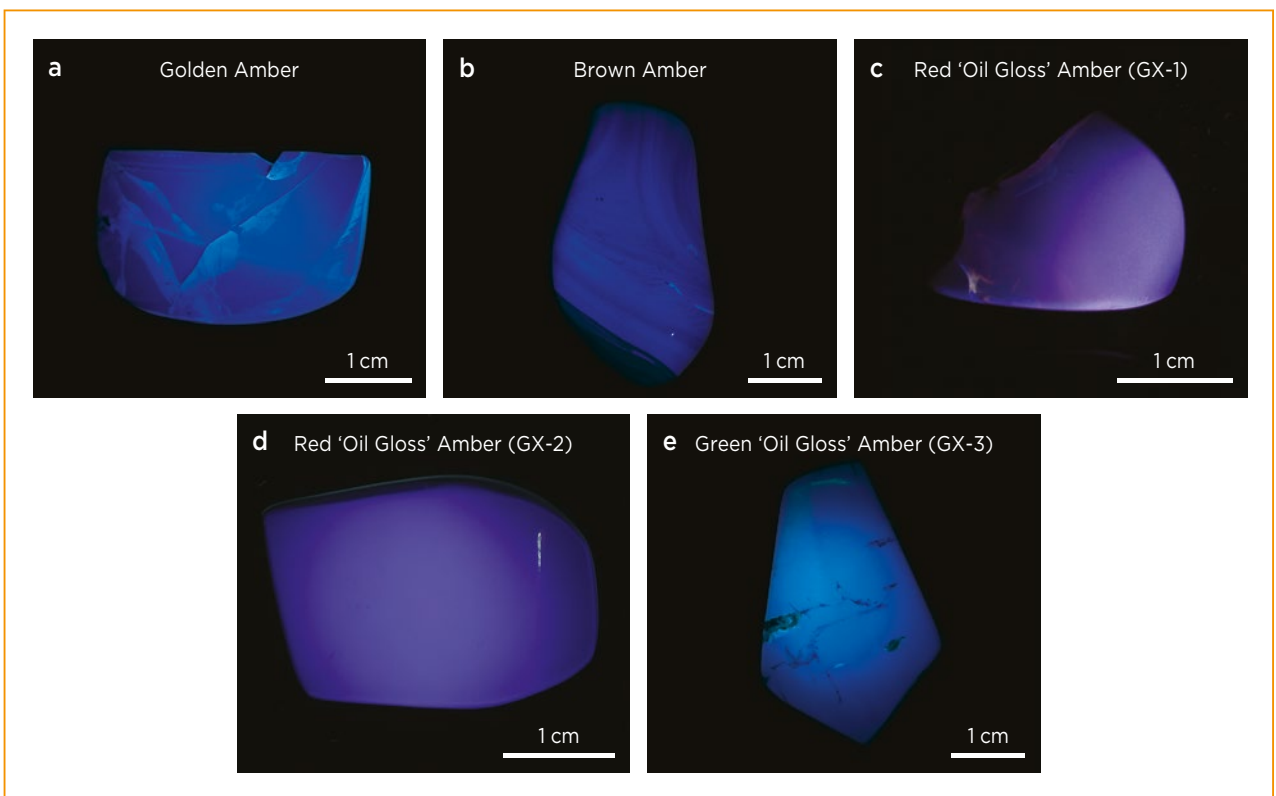
Figure 14: Viewed with long-wave UV fluorescence, Burmese amber typically fluoresces violetish blue (**a** and **b**). Less commonly, it displays magenta (**c**), violetish purple (**d**) or whitish blue (**e**) luminescence. Photos by X. Jiang.

Fluorescence Spectroscopy. Fluorescence spectra obtained for the golden and brown samples, as well as the three ambers showing the 'oil gloss' effect, recorded various luminescence centres (Figures 15–18 and Table II). Two luminescence centres in the 320–350 nm range fell outside the r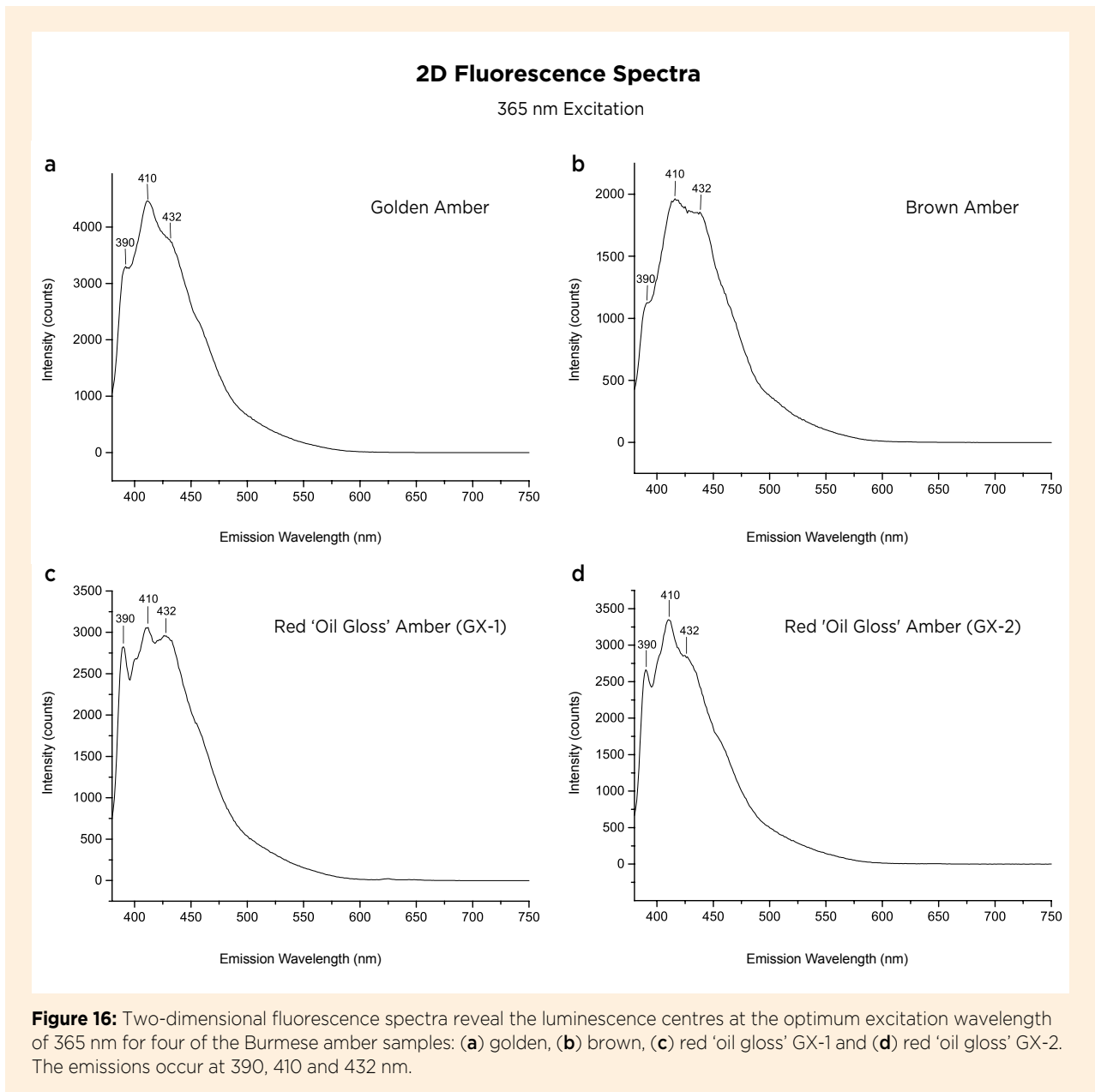ange of visible light. Other luminescence centres at 390 (±3) nm, 410 (±2) nm, 432 (±3) nm and 470 (±4) nm in the violet-to-blue region of the spectrum were recorded in all samples except for the amber displaying green 'oil gloss'. By contrast, the green 'oil gloss' sample showed emissions in the green region with increasing excitation wavelength (Figure 15e).
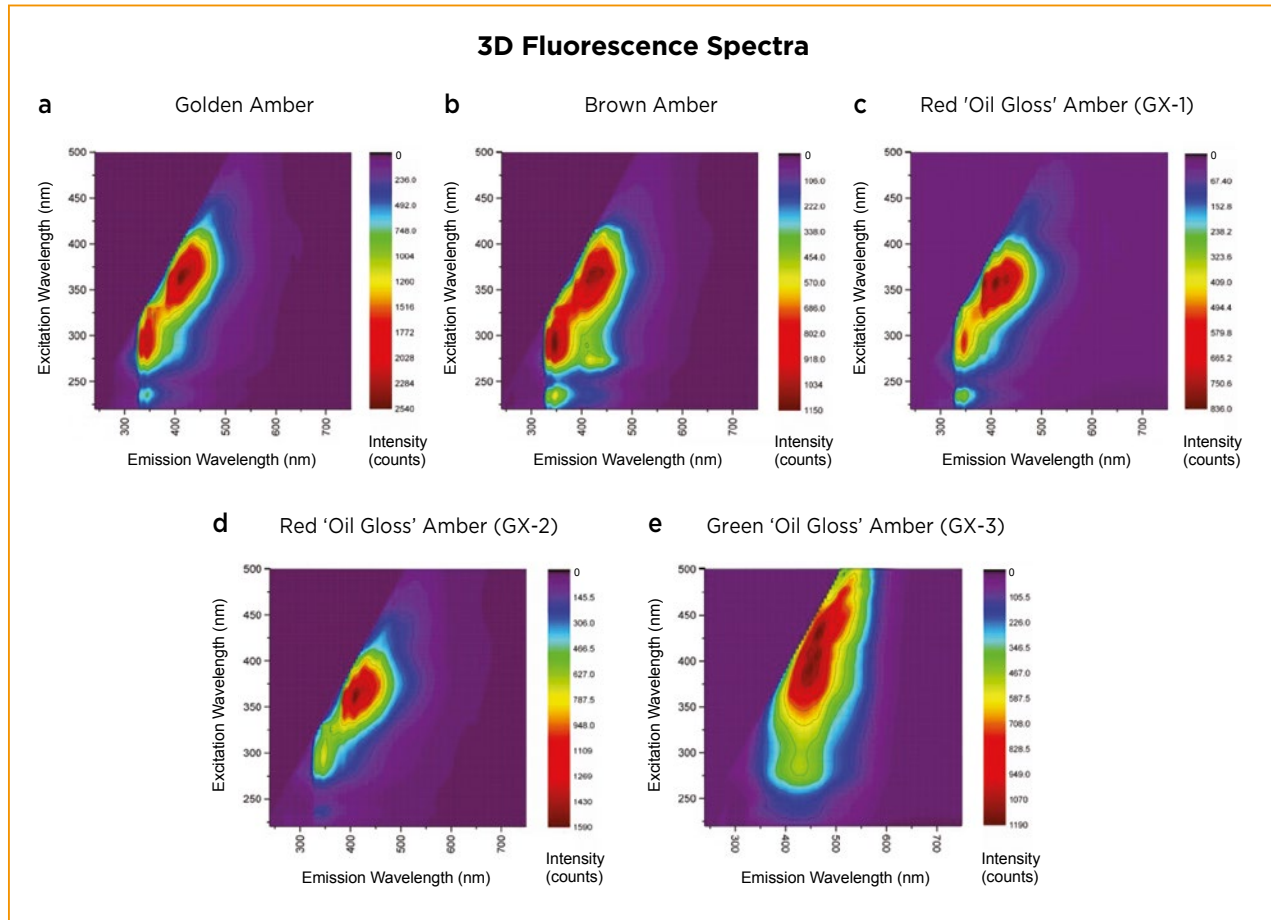
Figure 15: Three-dimensional fluorescence spectra are shown for the five Burmese amber samples in Figure 14: (**a**) golden, (**b**) brown, (**c**) red 'oil gloss' GX-1, (**d**) red 'oil gloss' GX-2 and (**e**) green 'oil gloss' GX-3. The spectra reveal luminescence centres at various wavelengths (see Table II for specific centres in each sample).

Table II: Long-wave UV fluorescence, luminescence centres (in the visible range) and phosphorescence lifetimes of Burmese amber.
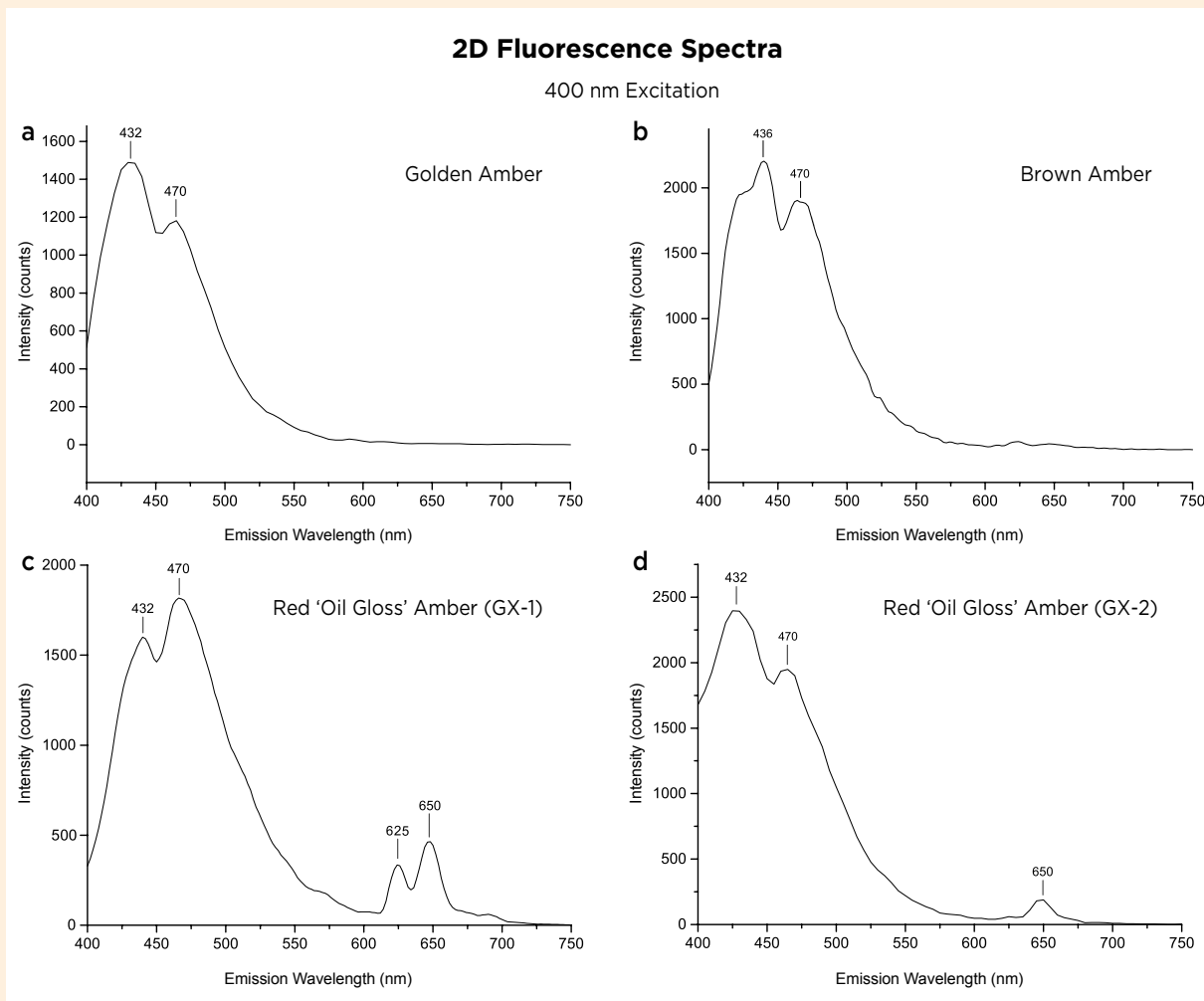
Sample ID	Type	Long-wave UV fluorescence	Luminescence centres (nm)	Phosphorescent lifetimes (s)
JP	Golden amber	Violetish blue	410, 432, 470	$t_1 = 0.375, t_2 = 1.396$
ZP	Brown amber	Violetish blue	410, 432, 470	$t_1 = 0.265, t_2 = 1.059$
GX-1	Red 'oil gloss'	Magenta	410, 432, 470, 625, 650	$t_1 = 0.134, t_2 = 0.447$
GX-2	Red 'oil gloss'	Violetish purple	410, 432, 470, 650	$t_1 = 0.154, t_2 = 0.607$
GX-3	Green 'oil gloss' (or 'chameleon')	Whitish blue	432, 470, 503, 532	$t_1 = 0.134, t_2 = 0.706$

Figure 16: Two-dimensional fluorescence spectra reveal the luminescence centres at the optimum excitation wavelength of 365 nm for four of the Burmese amber samples: (**a**) golden, (**b**) brown, (**c**) red 'oil gloss' GX-1 and (**d**) red 'oil gloss' GX-2. The emissions occur at 390, 410 and 432 nm.
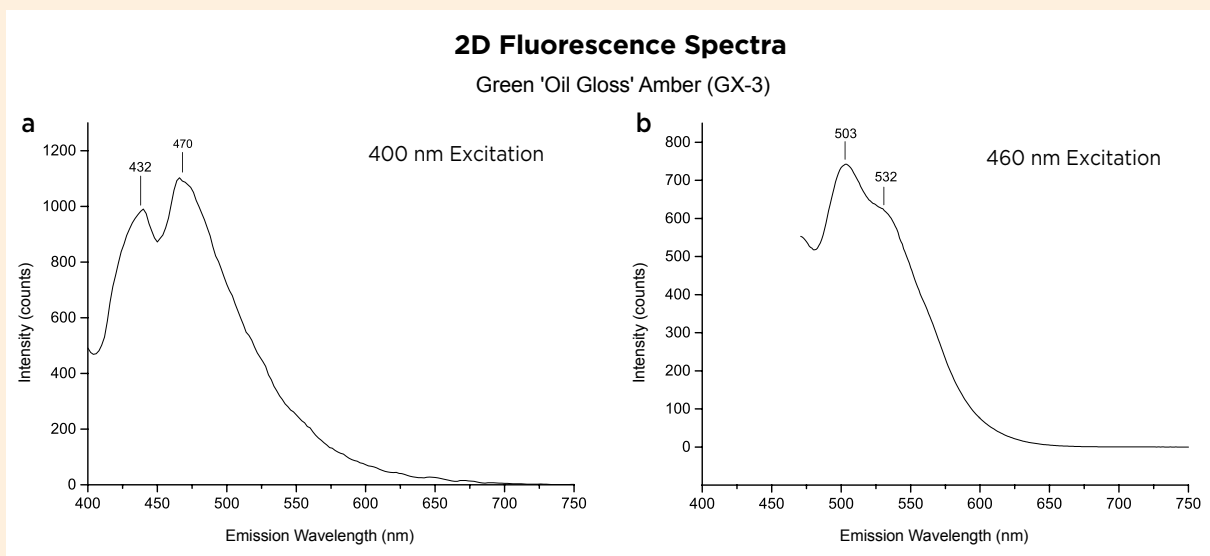
Two-dimensional fluorescence spectra were generated for the optimum excitation wavelength, which was 365 nm for all samples except for the amber showing green 'oil gloss' (which had an optimum excitation of 400 nm). With 365 nm excitation, the spectra showed luminescence centres at about 390, 410 and 432 nm (Figure 16). When the excitation wavelength was increased to 400 nm (i.e. in the visible range), a luminescence centre in the blue region at 470 nm appeared (Figure 17). Moreover, with 400 nm excitation the two red 'oil gloss' ambers also showed luminescence in the red region at 650 nm (±2 nm) and also at 625 nm for sample GX-1. For the green 'oil gloss' amber, the optimum excitation wavelength of 400 nm generated emissions at about 432 and 470 nm

(Figure 18a). At a higher excitation wavelength of 460 nm (i.e. further into the visible region), the luminescence centres shifted to the 500–550 nm range in the green portion of the spectrum (Figure 18b).
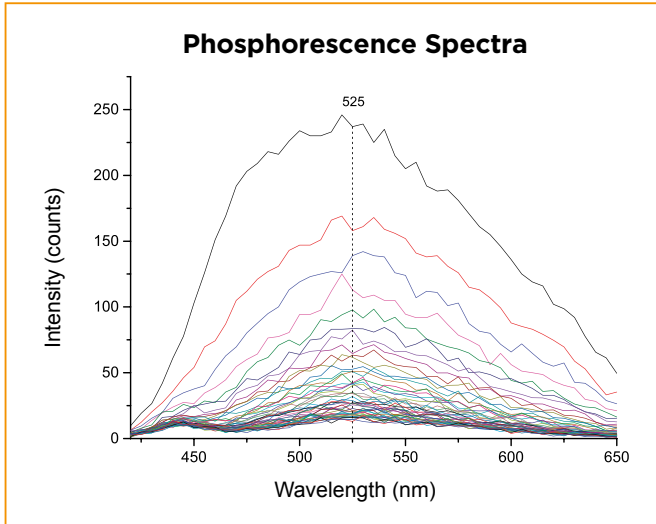
Phosphorescence Spectroscopy. Transient time-resolved phosphorescence spectroscopy showed that the strongest phosphorescence occurred at 525 nm (Figure 19) for all samples. Thus, the phosphorescence lifetime was measured for an emission wavelength of 525 nm and calculated using the decay function of Wang (2015). The results revealed two phosphorescence lifetimes for all the samples, with t_1 ranging from 0.134 to 0.375 s and t_2 ranging from 0.447 to 1.396 s (Figure 20; see Table II for details).

2D Fluorescence Spectra

400 nm Excitation

a Golden Amber

b Brown Amber

c Red 'Oil Gloss' Amber (GX-1)

d Red 'Oil Gloss' Amber (GX-2)

Figure 17: Two-dimensional fluorescence spectra of the same samples as in Figure 16 with 400 nm excitation show luminescence centres at 432 and 470 nm. In addition, red 'oil gloss' samples GX-1 and GX-2 have emission(s) in the red region at 650 nm ± 625 nm.

2D Fluorescence Spectra

Green 'Oil Gloss' Amber (GX-3)

a 400 nm Excitation

b 460 nm Excitation

Figure 18: Two-dimensional fluorescence spectra are shown for green 'oil gloss' amber GX-3. (**a**) At the optimum excitation wavelength of 400 nm, the luminescence centres occur only at 432 and 470 nm in the violet-to-blue region. (**b**) With 460 nm excitation, luminescence centres are revealed in the green region at 503 and 532 nm.

Figure 19: Time-resolved phosphorescence spectra demonstrate that the strongest phosphorescence occurred at 525 nm in all the Burmese amber samples. Each line refers to a different excitation wavelength.
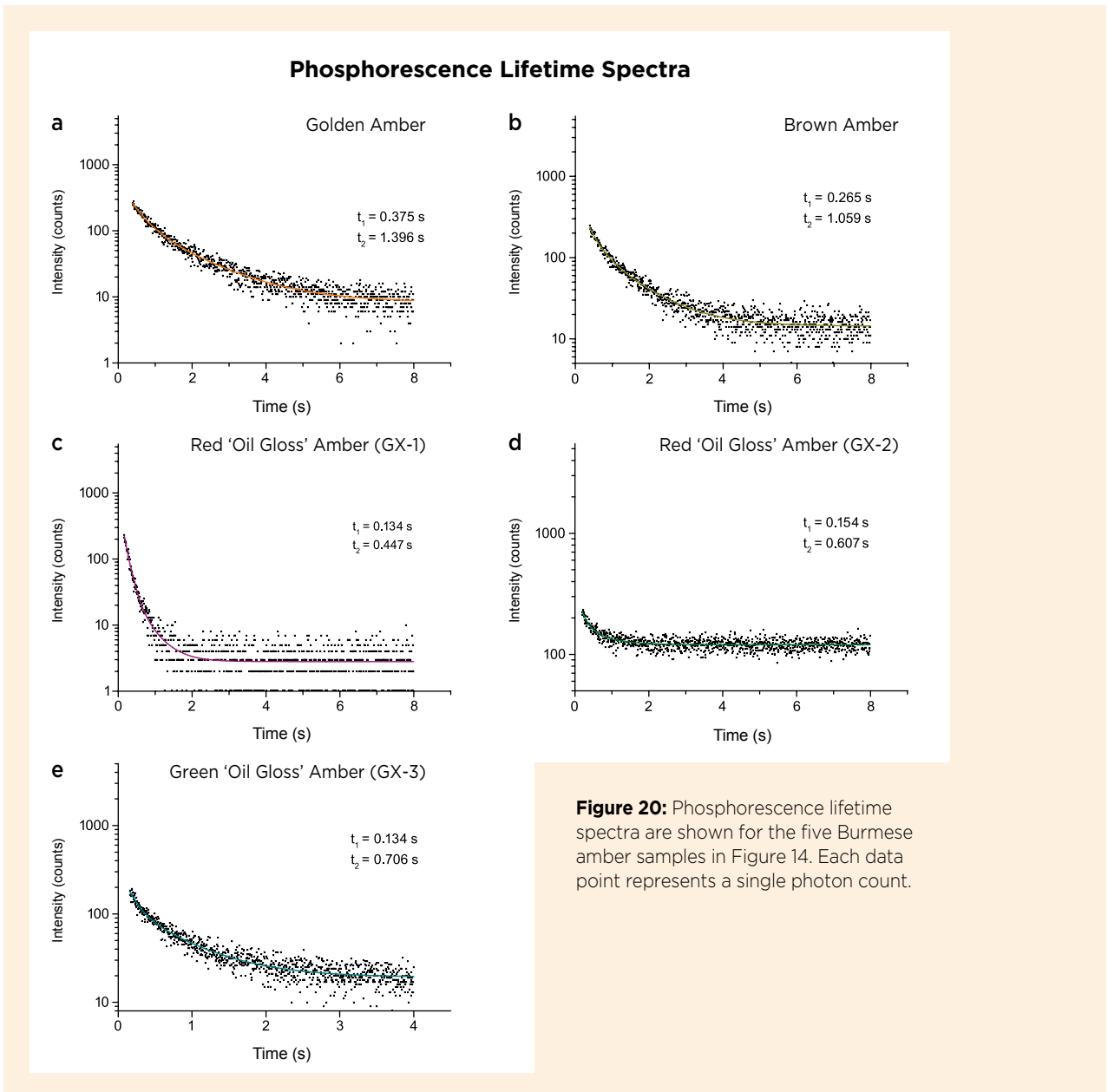
Figure 20: Phosphorescence lifetime spectra are shown for the five Burmese amber samples in Figure 14. Each data point represents a single photon count.

DISCUSSION

Formation of the Reddish Brown Dot-like Inclusions

The reddish brown dot-like inclusions in the brown amber (Figure 7c) showed a scaly structure in SEM images (Figure 9) that was clearly different from that of the surrounding amber. We speculate that these inclusions are related to some type of organic matter contained in the amber (especially volatile substances), rather than inorganic foreign material. Specifically, the inclusions may correspond to devolatilised sporopollen (chemically inert biological polymers) that were subjected to oxidation, thereby leading to a reddish brown appearance.

Structure of 'Root' Amber

According to our observations with the SEM, the diameter of the bubbles in the Burmese 'root' amber samples was micron-sized, typically ranging from 1 to 5.5 µm. In sample GP-1, an opaque region measuring 0.03 mm^2 contained 435 bubbles which took up 4.9% of the area. In the same region, hollow tubes occupied 257.1 µm^2. In the transitional zone leading into a transparent area, another 0.03 mm^2 region contained 149 bubbles of 0.9–5.5 µm diameter, which accounted for 3.1% of the area, and the hollow micro-tubes occupied 56.7 µm^2. Bubbles and hollow tubes were not present in the transparent zone. For sample GP-2, a 0.03 mm^2 region contained 47 bubbles which took up 1.8% of the area, but no hollow tubes. Thus, 'root' amber samples GP-1 and GP-2 differed considerably in their microscopic structural characteristics, and we attribute the distinctive textures seen in 'root' amber to variations in these structures.

The hollow micro-tubes accompanying the bubbles in 'root' amber GP-1 might represent escape channels for volatile components. The empty bubbles visible at the ends of the hollow tubes could have been left over when volatile components escaped along the tubes. The lack of bubbles visible at the ends of some tubes does not necessarily indicate an absence of bubbles, but may simply be due to the single plane being observed. The hollow tubes could also be related to cracks that appeared as the resin was exuded. The resin that formed Burmese amber was highly viscous, and as it was secreted in stages, small cracks could have resulted from more rapid hardening at the surface. However, the cracks could not continue to spread owing to rapid coverage by newly exuded resin. The 'internal' cracks were subsequently subjected to geological processes during burial of the host sediments. During this process, the healed fissures could have become channelways for escaping volatile components. Bubbles that remained after the volatiles escaped were mostly found along the curving, hollow tubes.

Origin of the 'Oil Gloss' Effect

The 'oil gloss' appearance of the Burmese amber is caused by a mixture of surface fluorescence and body colour, as seen in samples GX-1, GX-2 and GX-3. The effect is best seen against a black background because it reduces the influence of a sample's body colour on colour perception. The different appearances of this effect (red vs. green) depend on the luminescence centres present in the amber.

Amber with Red 'Oil Gloss'. Red surface fluorescence was noted on reddish brown and greenish yellow samples GX-1 and GX-2, respectively, when they were viewed against a black background. As expected, both showed emission in the red region at 650 nm (and also at 625 nm in GX-1) with 400 nm excitation (Figure 17c, d). Although this red emission was not recorded at the optimum excitation wavelength of 365 nm, it was present at a higher excitation wavelength in the range of visible light (i.e. 400 nm), and therefore we suggest that the red surface fluorescence of Burmese amber is related to these luminescence centres.

Nevertheless, the two samples showing the red 'oil gloss' effect also had strong luminescence centres in the violet-to-blue region at 432 and 470 nm, raising the question of how the 625 and 650 nm luminescence centres contribute to the red fluorescence. However, two-dimensional fluorescence spectroscopy of these samples using the Qspec micro-PL spectrometer (405 nm excitation) revealed that the red luminescence centres at 625 and 650 nm in GX-1 were stronger than the blue luminescence centres, and an additional red luminescence centre was also present at 690 nm (Figure 21a). In GX-2, the luminescence centres in the red region were nearly the same strength as those in the violet-to-blue region (Figure 21b). Therefore, it appears that different instruments have different sensitivities according to various emission wavelengths.

Amber with Magenta or Violetish Purple Fluorescence. Burmese amber commonly fluoresces violetish blue to long-wave UV radiation (e.g. Figure 14a). However, samples showing red 'oil gloss' showed magenta or violetish purple fluorescence under long-wave UV radiation (Figure 14c, d). Therefore, the luminescent centre(s) in the red region are not only responsible for the red 'oil gloss' effect, but they also contribute to the
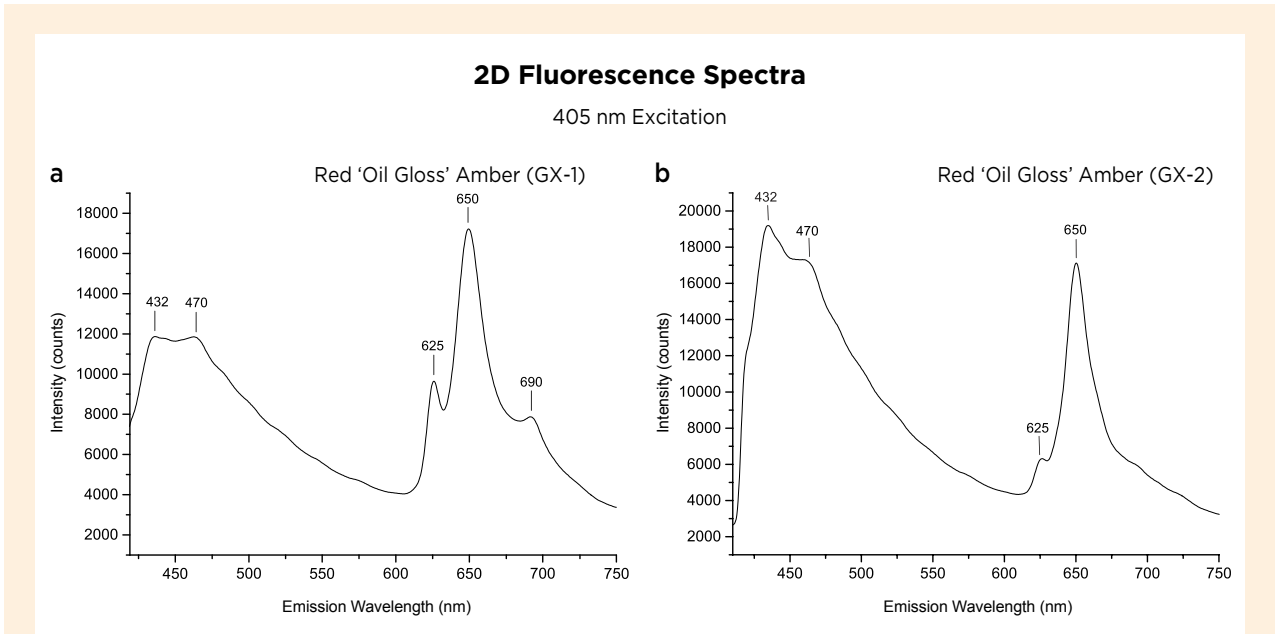
Figure 21: Two-dimensional fluorescence spectroscopy using the Qspec micro-PL instrument (405 nm excitation) shows luminescence centres in (**a**) red 'oil gloss' sample GX-1, which are much stronger in the red region at 625–690 nm than in the violet-to-blue region at 432 and 470 nm. (**b**) Red 'oil gloss' sample GX-2 shows strong emissions in both the violet-to-blue and red regions, but lacks a well-defined luminescence centre at 690 nm.

magenta or violetish purple fluorescence seen under long-wave UV radiation. The combination of luminescence centres in the red and violet-to-blue regions appears to be responsible for the distinctive magenta or violetish purple fluorescence of those samples seen under long-wave UV radiation.

Amber with Green 'Oil Gloss'. Reddish brown amber sample GX-3 displayed green surface fluorescence when viewed on a black background. In addition to the luminescence centres at 432 and 470 nm, fluorescence spectroscopy also revealed emissions in the green region (again, see Figure 18b). The spectral data were converted into Commission Internationale de L'Eclairage (CIE) chromaticity coordinate points, but the corresponding fluorescence did not plot in the green area—rather it plotted in the blue region (Figure 22). This suggests that the green 'oil gloss' of sample GX-3 is not only derived from green luminescence centres, but is also enhanced by the mixture of blue fluorescence and the amber's reddish brown body colour.

Phosphorescent Amber

'Glow in the dark' Burmese amber shows phosphorescence. With an excitation wavelength of 365 nm (typical long-wave UV radiation), the phosphorescent luminescence centre with the highest intensity was at 525 nm (yellowish green area of the spectrum), which is similar to the visually observed greenish yellow phosphorescent colour of Burmese amber. Thus, we measured the phosphorescence lifetime at 525 nm.

Phosphorescence lifetime is defined as the time it takes for the phosphorescence to decrease to 36.8% of the maximum strength (i.e. one lifetime), rather than the
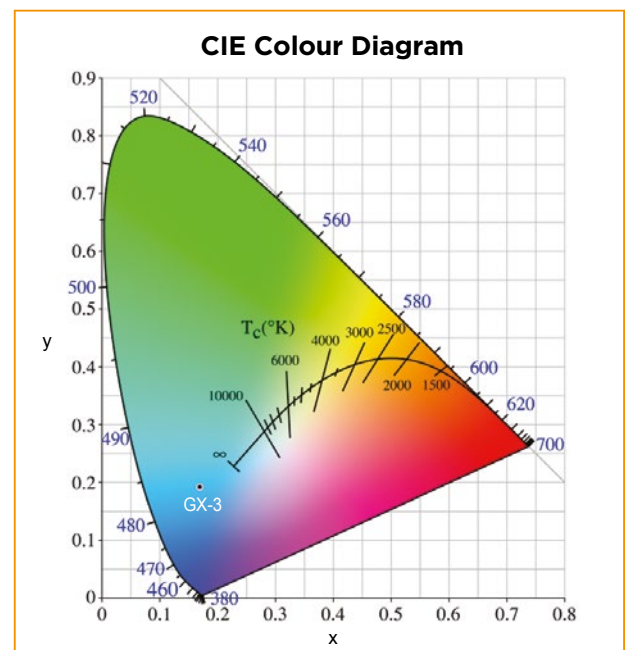
Figure 22: The CIE coordinate point calculated from the spectral data for green 'oil gloss' amber sample GX-3 confirmed the fluorescence colour as blue.

time to disappearance (when it becomes invisible to the naked eye; for more information, see Díaz García & Badía 2006). After phosphorescent amber is exposed to bright light, a large number of photons are emitted, leading to luminescence. The higher the intensity of the excitation source and the longer the exposure time, the more photons are excited in this process, resulting in longer times of luminescent energy emission. Hence, longer duration and higher intensity of irradiation contribute to longer 'luminescence times' (Xia 1992). However, after sufficient exposure time, regardless of how much longer the excitation lasts, the phosphorescence lifetime will remain nearly the same. This indicates a threshold inherent in the amber phosphorescence phenomenon. Once the quantity of excited photons reaches the threshold, the total number of active photons does not increase. At that point, the absorption and release of luminescent energy strike a dynamic balance.

Among the large number of organic compounds that are known to occur in amber, only a few can emit strong fluorescence, which is closely associated with their structures. Amber is a mixture of organic compounds, and may display fluorescence and sometimes phosphorescence when it contains the appropriate natural fluorescent impurities (e.g. Chekryzhov *et al.* 2014). Although Burmese amber is commonly thought to be the only fossil resin that displays the 'glow-in-the-dark' phenomenon, in fact amber from many origins may emit phosphorescence (e.g. Dominican amber; see Liu *et al.* 2014). The results of the authors' investigations of phosphorescence in ambers from various localities will be published in the future.

Figure 23: This Burmese amber carving depicts a *lohan* from traditional Chinese mythology. The amber displays a green 'oil gloss' effect in the transparent part, whereas the opaque areas consist of 'root' amber. The amber is 20.5 cm wide and rests on a carved wooden stand. Photo courtesy of Tengchong Huo Ren Carving Studio.

CONCLUSIONS

We characterised various types of Burmese amber, including golden, brown, 'blood', 'beeswax' and 'root' varieties, as well as those showing 'oil gloss' surface fluorescence effects and phosphorescence. Differences in the original resin secretions are responsible for the different amber types, as evidenced by the layered structure of some specimens and the characteristics of bubbles of various sizes and concentrations. It is also possible for multiple types/phenomena to occur within a single piece of Burmese amber (e.g. Figure 23).

The reddish brown dot-like inclusions in brown Burmese amber are possibly related to reactions involving volatile substances. The association of these inclusions with flow patterns suggests they may be related to the escape of volatile components. The opaque appearance

of Burmese 'root' amber is primarily attributed to its layered microscopic structure, as well as the abundance of bubbles and microscopic hollow tubes in certain areas of this material. The micro-tubes may have formed as escape channels for volatile components or they may be related to small cracks that formed during more rapid hardening of the outer surface of the resin and were then covered by successive resin exudations.

Red or green 'oil gloss' effects in Burmese amber are produced by a mixture of surface fluorescence and body colour, while the 'glow-in-the-dark' phenomenon is produced by phosphorescence. Generally, Burmese amber has two luminescence centres in the violet-to-blue region (at 432 and 470 nm), and those samples displaying red 'oil gloss' show additional emission(s) in the red region at 625–690 nm.

An important challenge facing amber researchers is the identification of specific components and structural formulas in these materials, and this investigation of the fluorescence and phosphorescence of Burmese amber not only explains various distinctive appearances shown by this material, but also provides further information for future research on the organic components in amber.

REFERENCES

Abduriyim, A., Kimura, H., Yokoyama, Y., Nakazono, H., Wakatsuki, M., Shimizu, T., Tansho, M. & Ohki, S. 2009. Characterization of "green amber" with infrared and nuclear magnetic resonance spectroscopy. *Gems & Gemology*, **45**(3), 158–177, https://doi.org/10.5741/gems.45.3.158.

Chekryzhov, I.Y., Nechaev, V.P. & Kononov, V.V. 2014. Blue-fluorescing amber from Cenozoic lignite, eastern Sikhote-Alin, Far East Russia: Preliminary results. *International Journal of Coal Geology*, **132**, 6–12, https://doi.org/10.1016/j.coal.2014.07.013.

Cruickshank, R.D. & Ko, K. 2003. Geology of an amber locality in the Hukawng Valley, northern Myanmar. *Journal of Asian Earth Sciences*, **21**(5), 441–455, https://doi.org/10.1016/s1367-9120(02)00044-5.

Díaz García, M.E. & Badía, R. 2006. Phosphorescence measurements, applications of. *In*: Meyers, R.A. (ed), *Encyclopedia of Analytical Chemistry*, John Wiley & Sons Ltd, New York, New York, USA, 14 pp., https://doi.org/10.1002/9780470027318.a5411.

Dutta, S., Mallick, M., Kumar, K., Mann, U. & Greenwood, P.F. 2011. Terpenoid composition and botanical affinity of Cretaceous resins from India and Myanmar. *International Journal of Coal Geology*, **85**(1), 49–55, https://doi.org/10.1016/j.coal.2010.09.006.

Edwards, H.G.M., Farwell, D.W. & Villar, S.E.J. 2007. Raman microspectroscopic studies of amber resins with insect inclusions. *Spectrochimica Acta Part A: Molecular and Biomolecular Spectroscopy*, **68**(4), 1089–1095, https://doi.org/10.1016/j.saa.2006.11.037.

Jiang, W., Nie, S. & Wang, Y. 2017. Fluorescence spectral characteristic of blue amber from Dominican Republic, Mexico and Myanmar. *Journal of Gems and Gemology*, **19**(2), 1–8 (in Chinese with English abstract).

Jiang, X., Wang, Y. & Kong, F. 2018. Microstructure characteristic of amber from Myanmar. *Journal of Gems and Gemology*, **20**(6), 18–30 (in Chinese with English abstract).

Jiang, X., Zhang, Z., Wang, Y. & Kong, F. 2019. Special optical effect of amber from Myanmar. *Journal of Gems and Gemology*, **21**(5), 1–17 (in Chinese with English abstract).

Lambert, J.B. & Frye, J.S. 1982. Carbon functionalities in amber. *Science*, **217**(4554), 55–57, https://doi.org/10.1126/science.217.4554.55.

Lan, J., Lan, Y., Hu, C. & Li, X. 2017. Application of GC-MC and FTIR in identification of amber and copal resin. *Journal of Gems and Gemology*, **19**(2), 9–19 (in Chinese with English abstract).

Laurs, B.M. 2012. Gem News International: Burmese amber update. *Gems & Gemology*, **48**(2), 142–155, https://doi.org/10.5741/gems.48.2.142.

Levinson, A.A. 2001. Gem News International—Amber ("Burmite") from Myanmar: Production resumes. *Gems & Gemology*, **37**(2), 142–143.

Liu, S.I 2018. Gem Notes: Burmese amber from Khamti, Sagaing region. *Journal of Gemmology*, **36**(2), 107–110.

Liu, Y., Shi, G. & Wang, S. 2014. Color phenomena of blue amber. *Gems & Gemology*, **50**(2), 134–140, https://doi.org/10.5741/gems.50.2.134.

Lu, B., Yang, D., Fang, H. & Shi, G. 2014. A preliminary study of inclusions in the burmite (Myanmar amber) and their significance. *Acta Petrologica et Mineralogica*, **33**(Supp. 2), 117–122 (in Chinese with English abstract).

Marrison, L.W. 1951. Characteristic absorption bands in the 10-μ region of the infra-red spectra of *cyclo*Paraffin derivatives. *Journal of the Chemical Society (Resumed)*, 1614–1617, https://doi.org/10.1039/jr9510001614.

Shi, G., Grimaldi, D.A., Harlow, G.E., Wang, J., Wang, J., Yang, M., Lei, W., Li, Q. *et al.* 2012. Age constraint on Burmese amber based on U–Pb dating of zircons. *Cretaceous Research*, **37**, 155–163, https://doi.org/10.1016/j.cretres.2012.03.014.

Tay, T.S., Kleišmantas, A., Nyunt, T.T., Minrui, Z., Krishnaswamy, M. & Ying, L.H. 2015. Burmese amber from Hti Lin. *Journal of Gemmology*, **34**(7), 606–615, https://doi.org/10.15506/JoG.2015.34.7.606.

Wang, P. 2015. Process the experimental data of time-resolved photoluminescence lifetime spectra of Cu$_2$O nanowires by origin. *Physical Experiment of College*, **28**(3), 80–83 (in Chinese with English abstract).

Wang, Y. 2018. *Amber Gemology*. China University of Geosciences Press, Beijing, China, 244 pp. (in Chinese).

Wang, Y., Shi, G., Shi, W. & Wu, R. 2015. Infrared spectral characteristics of ambers from three main sources (Baltic, Dominica and Myanmar). *Spectroscopy and Spectral Analysis*, **35**(8), 2164–2169 (in Chinese with English abstract).

Wang, Y., Wang, Q. & Nie, S. 2016. Gas bubble characteristic of translucent to opaque amber and its relationship to quality assessment. *Journal of Gems & Gemmology*, **18**(5), 20–27 (in Chinese with English abstract).

Wang, Y., Yang, M., Nie, S. & Liu, F. 2017. Gemmological and spectroscopic features of untreated vs. heated amber. *Journal of Gemmology*, **35**(6), 530–542, https://doi.org/10.15506/JoG.2017.35.6.530.

Xia, J. 1992. *Practical Fluorescence Analysis*. Chinese People's Public Security University Press, Beijing, China, 335 pp. (in Chinese).

Xiao, R. & Kang, J. 2018. Characteristics of Burma blood amber and other colours of ambers. *Superhard Material Engineering*, **30**(2), 54–58 (in Chinese with English abstract).

Xiao, Y., Guo, Y. & Chen, D.P. 2014. The influences of lightness variation of the non-color background on the color of the blood amber. *Key Engineering Materials*, **633**, 524–535, https://doi.org/10.4028/www.scientific.net/KEM.633.524.

Xie, X., Di, J. & Wu, X. 2017. Type of amber from Myanmar and its gemmological characteristic. *Journal of Gems and Gemmology*, **19**(5), 48–59 (in Chinese with English abstract).

Xing, L., McKellar, R.C., Wang, M., Bai, M., O'Connor, J.K., Benton, M.J., Zhang, J., Wang, Y. *et al.* 2016. Mummified precocial bird wings in mid-Cretaceous Burmese amber. *Nature Communications*, **7**(1), article 12089 (7 pp.), https://doi.org/10.1038/ncomms12089.

Zhang, X. & Li, R. 2010. Principle of SEM and application in TFT-LCD production. *Advanced Display*, **21**(1), 10–15 (in Chinese with English abstract).

Zhang, Z., Lin, Q. & Shen, A. 2017. Characteristic of oxygen content in black amber from Myanmar. *Journal of Gems & Gemmology*, **19**(1), 17–21 (in Chinese with English abstract).

Zherikhin, V.V. & Ross, A.J. 2000. A review of the history, geology and age of Burmese amber (Burmite). *Bulletin of the Natural History Museum* [London], *Geology Series*, **56**(1), 3–10.

Zong, P., Xue, J. & Tang, B. 2014. Tracing the most ancient amber: The origin and evolution of resin-producing plants. *Acta Petrologica et Mineralogica*, **33**(S2), 111–116 (in Chinese with English abstract).

The Authors

Xinran Jiang, Zhiqing Zhang and Dr Yamei Wang
Gemmological Institute, China University of Geosciences, No. 388 Lumo Rd., 430074 Wuhan, China
Email: wangym@cug.edu.cn

Fanli Kong
Century Amber Museum, 1 Songrui Road, Songgang, Baoan District, Shenzhen, China